



UNIVERSIDAD REGIONAL AMAZÓNICA IKIAM

FACULTA DE CIENCIAS DE LA TIERRA Y AGUA

CARRERA DE GEOCIENCIAS

**ESTIMACIÓN DE LA TASA ANUAL DE ACUMULACIÓN DE
MICROPLÁSTICOS EN UN GLACIAR ANDINO TROPICAL. CASO DE
ESTUDIO: GLACIAR ANTISANA**

Proyecto de investigación previo a la obtención del título de:

Ingeniera en Geociencias.

AUTOR: JULIETH ESTHER CHANCAY SÁNCHEZ

TUTOR: PhD BRYAN GUIDO VALENCIA CASTILLO

Tena – Ecuador

2024

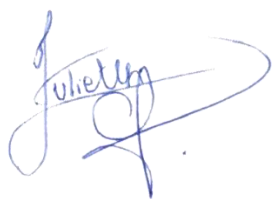
Carrera de Geociencias

Declaración de derecho de autor, autenticidad y responsabilidad

Tena, 16 de agosto del 2024

Yo, Julieth Esther Chancay Sánchez con documento de identidad 1350579981 declaro que los resultados obtenidos en la investigación que presento en este documento final, previo a la obtención del título de Ingeniera en Geociencias, son absolutamente inéditos, originales, auténticos y personales.

En virtud de lo cual, el contenido, criterios, opiniones, resultados, análisis, interpretaciones, conclusiones, recomendaciones y todos los demás aspectos vertidos en el presente documento, son de mi autoría y de mi absoluta responsabilidad.



Julieth Esther Chancay Sánchez.

CI: 1350579981

Carrera de Geociencias

Autorización de publicación en el Repositorio Institucional

Tena, 16 de agosto del 2024

Yo, Julieth Esther Chancay Sánchez, con documento de identidad 1350579981 en calidad de autor/a y titular de los derechos morales y patrimoniales del trabajo de titulación “Estimación de la tasa anual de acumulación de microplásticos en un glaciar andino tropical. Caso de estudio: glaciar Antisana”, de conformidad con el Art. 114 del CÓDIGO ORGÁNICO DE LA ECONOMÍA SOCIAL DE LOS CONOCIMIENTOS, CREATIVIDAD E INNOVACIÓN, reconozco a favor de la Universidad Regional Amazónica Ikiam una licencia gratuita, intransferible y no exclusiva para el uso no comercial de la obra, con fines estrictamente académicos.

Así mismo autorizo a la Universidad Regional Amazónica Ikiam para que realice la publicación de este trabajo de titulación en el Repositorio Institucional de conformidad a lo dispuesto en el Art. 144 de la Ley Orgánica de Educación Superior.



Julieth Esther Chancay Sánchez

CI: 1350579981

Carrera de Geociencias

Certificado de dirección de trabajo de titulación

Certifico que el trabajo de titulación: “Estimación de la tasa anual de acumulación de microplásticos en un glaciar andino tropical. Caso de estudio: glaciar Antisana”, aprobado bajo el mecanismo de titulación de: artículo, fue realizado por Julieth Esther Chancay Sánchez, bajo mi dirección.

El mismo ha sido revisado en su totalidad y analizado por la herramienta de verificación de similitud de contenido; por lo tanto, cumple con los requisitos teóricos, científicos, técnicos, metodológicos y legales establecidos por la Universidad Regional Amazónica Ikiám, para su entrega y defensa.

Tena, 16 de agosto del 2024



Bryan Guido Valencia Castillo
C.I: 1760101632
Tutor

AGRADECIMIENTO

Quiero expresar mi más profundo agradecimiento a mi familia, cuyo inquebrantable apoyo ha sido la fuerza que me ha impulsado a alcanzar mis metas. A mi madre, Miriam Sánchez, por su presencia constante y amorosa; a mi padre, Wilmer Chancay, por sus palabras de aliento que siempre han iluminado mi camino; a mi hermano, Juseth Chancay, por enseñarme el valor del esfuerzo perseverante; y a mi querida Pucka, cuya leal dulzura ha sido un consuelo en cada momento.

Extiendo mi gratitud a mis profesores, Bryan Valencia, Oswaldo Guzmán y Corina Campos, quienes me han inspirado a ser una persona soñadora y crítica, y que, en los momentos de duda, me han ayudado a creer en mí misma. A mis amigos Luis Andrés, Dimas, Isaac, Alex, Shyrma y Joselin, gracias por llenar de alegría mis días más difíciles.

DEDICATORIA

A mi familia, Miriam, Wilmer y Juseth, por ser el ancla en mi vida, por enseñarme que el amor y la unión son la verdadera fuerza detrás de cualquier éxito. Este logro es tan suyo como mío, porque sin ustedes, el camino habría sido imposible.

TABLA DE CONTENIDO

Portada	
Declaración de derecho de autor, autenticidad y responsabilidad.....	ii
autorización de publicación en el repositorio institucional	iii
Certificado de dirección de trabajo de titulación	iv
Agradecimiento.....	v
Dedicatoria.....	vi
Índice de figuras.....	viii
Resumen	ix
Abstract.....	x
1. Introducción.....	2
2. Métodos.....	5
2.1 Área de estudio.....	5
2.2 Recolección de muestras	6
2.3 Caracterización de polímeros	7
2.4 Separación de microplásticos	7
2.5 Modelo de edad.....	8
2.6 Análisis estadístico	9
3. Resultados.....	11
3.1 Edad del núcleo de hielo.....	11
3.2 Identificación y cuantificación de microplásticos.....	15
3.3 Tasa de acumulación de microplásticos	16
4. Discusión	17
5. Conclusión.....	21
6. Referencias.....	

ÍNDICE DE FIGURAS

Figure 1.2 Mapa del área de estudio	6
Figure 2.2 Regresión lineal..	10
Figure 3.3 Proceso de remuestreo de resolución de profundidad.....	12
Figure 4.3 Análisis Wavelet	13
Figure 5.3 Fluctuaciones isotópicas de $\delta^{18}\text{O}$	14
Figure 6.3 Clasificación de microplásticos por su forma	15
Figure 7.3 Clasificación y proporción de microplásticos por polímero	16
Figure 8.4 Diferencias entre las tasas de crecimiento de los microplásticos atmosféricos y microplásticos oceánicos.	18

RESUMEN

Los microplásticos (MPs) son fragmentos de plástico que varían en tamaño desde 5 hasta 0.001 mm y se han encontrado globalmente en ecosistemas terrestres y acuáticos. Su presencia en lugares remotos como el glaciar Antisana en los Andes tropicales sugiere un transporte atmosférico extenso. Sin embargo, el ritmo en el que los MPs aumentan en la atmósfera aún no ha sido estimado. Aquí presentamos el primer estudio que estima esta tasa de acumulación de MPs durante un año hidrológico mediante el análisis de un núcleo de hielo de 8 metros obtenido del glaciar 15- α del Volcán Antisana en Ecuador. Se cuantificó de manera visual la cantidad de MPs a lo largo del núcleo de hielo y se utilizó espectroscopía infrarroja por transformada de Fourier (FTIR) para identificar su composición. El núcleo de hielo de 8 metros representó aproximadamente 12 meses según el análisis isotópico de $\delta^{18}\text{O}$. Se emplearon técnicas de regresión lineal y bootstrap para estimar una tasa de acumulación anual del 5.84%, aumentando los MPs de 36 al inicio del año a 83 al final del mismo. Se cuantificaron un total de 1762 MPs, principalmente fibras, seguidas de fragmentos. Entre los polímeros identificados se encuentran polietileno, polimetilmetacrilato, copolímeros de Metacrilato de 2-(dimetilamino)etilo, poliéster, polietilenimina, poliamida, politetrafluoroetileno y polímeros celulósicos. Se concluyó que la cantidad de MPs es inversamente proporcional a la profundidad del núcleo de hielo, es decir, la cantidad de MPs fue más abundantes en las capas de hielo más jóvenes, indicando concentraciones más altas en niveles superficiales.

PALABRAS CLAVE: Microplásticos, Glaciares, Andes, Atmósfera, Contaminación.

ABSTRACT

Microplastics (MPs) are plastic fragments ranging in size from 5 to 0.001 mm and have been found globally in terrestrial and aquatic ecosystems. Their presence in remote locations such as the Antisana glacier in the tropical Andes suggests extensive atmospheric transport. However, the rate at which MPs increase in the atmosphere has not yet been estimated. This study presents the first estimation of this accumulation rate over a hydrological year through the analysis of an 8-meter ice core from the 15- α Glacier on the Antisana Volcano in Ecuador. The quantity of MPs along the ice core was visually quantified, and Fourier-transform infrared spectroscopy (FTIR) was used to identify their composition. The 8-meter ice core represented approximately 12 months according to $\delta^{18}\text{O}$ isotopic ice core analysis. Linear regression and bootstrap techniques were employed to estimate an annual accumulation rate of 5.84%. The amount of MPs increased from 36 at the start of the year to 83 by the end. A total of 1762 MPs were quantified, predominantly fibers followed by fragments. Identified polymers included polyethylene, polymethyl methacrylate, 2-(dimethylamino)ethyl methacrylate copolymers, polyester, polyethylenimine, polyamide, polytetrafluoroethylene, and cellulosic polymers. It was concluded that the amount of MPs is inversely proportional to the depth of the ice core, with higher concentrations of MPs in the younger ice layers, indicating greater abundance at surface levels.

KEYWORDS: Microplastics, Glaciers, Andes, Atmosphere, Pollution.

Journal Science of the Total Environment:

<https://www.sciencedirect.com/journal/science-of-the-total-environment>

**ESTIMATION OF THE ANNUAL MICROPLASTICS ACCUMULATION RATE IN A TROPICAL
ANDEAN GLACIER. CASE STUDY: ANTISANA GLACIER.**

1. INTRODUCTION

Microplastics (hereafter MPs) are plastic particles ranging in length from 5 to 0.001 mm (Andrady, 2011; Chandra & Walsh, 2024; Evangeliou et al., 2020; Otegui et al., 2024) that constitute long-lasting environmental pollutants with a diverse array of negative impacts on living organisms (Khoshmanesh et al., 2023; Mierzejewski et al., 2023; Rafa et al., 2024; Song et al., 2022). MPs pollution has become ubiquitous in populated areas (Allen et al., 2021; Chandrakanthan et al., 2024; Dhivert et al., 2024; Hurley et al., 2018), marine environments (Ding et al., 2022; X. Wang et al., 2020), and remote regions including Antarctica, the Alps, and Andean glaciers (Ambrosini et al., 2019; Bergmann et al., 2019; Cabrera et al., 2020; Gonzalez-Pleiter et al., 2021; Parolini et al., 2021; Scheurer & Bigalke, 2018). The dynamics of MPs in high mountain glaciers, such as the Antisana glacier in Ecuadorian Andes, are influenced by atmospheric transport, whereby airborne MPs are deposited in snow and accumulate in glacier ice through time (Cabrera et al., 2022; Fox et al., 2024; Sridharan et al., 2021; Ward et al., 2024; Wright et al., 2013).

Plastic production began in 1950 and increased to 400 million tons in 2023 (Andrady, 2011; Barnes et al., 2009; Walker & Fequet, 2023). If plastic production increases every year, the underlying assumption is that the amount of MPs found in terrestrial (Dissanayake et al., 2022; Surendran et al., 2023), marine (Hinata et al., 2023; Salomone et al., 2023), and cryospheric environments (Niu et al., 2024; Rosso et al., 2024; Zhang et al., 2020) is also increasing every year. While the presence and atmospheric transport of MPs in remote areas have been documented (Allen et al., 2019; Bank & Hansson, 2019; Cabrera et al., 2022; Fox et al., 2024; Zhang et al., 2020), the annual amount of MPs transported through the atmosphere and deposited in remote locations such as high mountain glaciers has not yet to be estimated.

Glaciers are potential sites for the accumulation of MPs because their transport involves moist air masses originating from the Atlantic Ocean that move from east to west,

crossing the Amazon rainforest until they meet the Andes mountain range, producing orographic precipitation over the glaciers (Ginot et al., 2010; Stansell et al., 2023; Vimeux et al., 2005; Vuille, 2023) and facilitating the accumulation of MPs. It has been observed that MPs can be transported from terrestrial or oceanic surfaces to remote locations through the atmosphere (Allen et al., 2019; Fox et al., 2024; K. Liu et al., 2019, 2020; Z. Liu et al., 2024; Martina & Trini Castelli, 2023). However, research has predominantly focused on documenting the presence of MPs in marine sediments, leaving a gap in understanding the amount of MPs accumulating in the atmosphere in relation to the increase of marine MPs.

MPs had previously been documented in glacier 15- α of Antisana Volcano in Ecuador (Cabrera et al., 2020, 2022); however, these studies focused on determining the abundance of MPs in the glacier's surface snow layer. This study is the first to analyze the continuous accumulation of atmospheric MPs over a hydrological year. Understanding the rate at which atmospheric MPs accumulate in high mountain glaciers is of utmost importance because, due to the melting of glaciers, accumulated MPs could be released into water bodies and reach natural urban water reservoirs (Zhang, 2019).

The consumption and inhalation of MPs generate adverse impacts on human health, such as lung inflammation, interference with normal cellular activity, and negative effects on human reproduction (Barceló et al., 2023; Koutnik et al., 2021; Polidoro et al., 2022). Additionally, MPs can absorb persistent organic pollutants and toxic additives, facilitating their transfer to humans (Cole et al., 2016). Low-density MPs, such as polyethylene (PE), tend to be transport over longer distances than high-density ones (Y. Wang & Chen, 2023), increasing the likelihood of their presence in the atmosphere. PE has been observed to cause allergies, asthma, and have carcinogenic potential (Isci & Dagdemir, 2024). Furthermore, PE can become contaminated with chemical additives during its manufacturing process, which, upon degradation, could pose a risk to human health and the environment (Cheshmazar et al., 2021).

In this study, we present the first investigation of MPs accumulation rates over time in an 8-meter ice core obtained from Glacier 15- α on the Antisana Volcano in Ecuador. We reveal the accumulation of MPs over a hydrological year. Our hypothesis is that the quantity of MPs will decrease with greater depth in the ice core, considering that the more superficial a layer of ice is, the more recent its deposition. Our findings show the proportion of MPs forms and polymers.

2. METHODS

2.1 Study area

Sampling was carried out on the 15- α glacier of the Antisana Volcano (0°28'S; 25 78°09'W) in the Ecuadorian Andes. The Antisana glacier (Figure 1) covers an approximate total area of 15 km² and reaches an elevation of 5753 meters above sea level (m.a.s.l) (Basantes-Serrano et al., 2016). The Antisana glaciers serve as a significant water source for the city of Quito, the capital of Ecuador. Additionally, runoff from the 15- α glacier contributes to the Antisana River, a tributary of the Amazon River system (Hall et al., 2017). Precipitation in the Antisana follows a bimodal seasonal cycle, with high precipitation peaks in the months of February to June and September to November (Basantes-Serrano et al., 2016). Moisture reaching the Antisana volcano originates from the Atlantic Ocean and is depleted of heavy $\delta^{18}\text{O}$ isotopes during the months of December, January, and February (Baker & Fritz, 2015). The average temperature above 4850 m.a.s.l ranges between 0°C and 2°C (Cauvy-Fraunié et al., 2013). The site where the ice core was collected is located above the equilibrium line altitude (ELA); therefore, snow ablation is a negligible process that may introduce an estimation bias when estimating the accumulation of MPs.

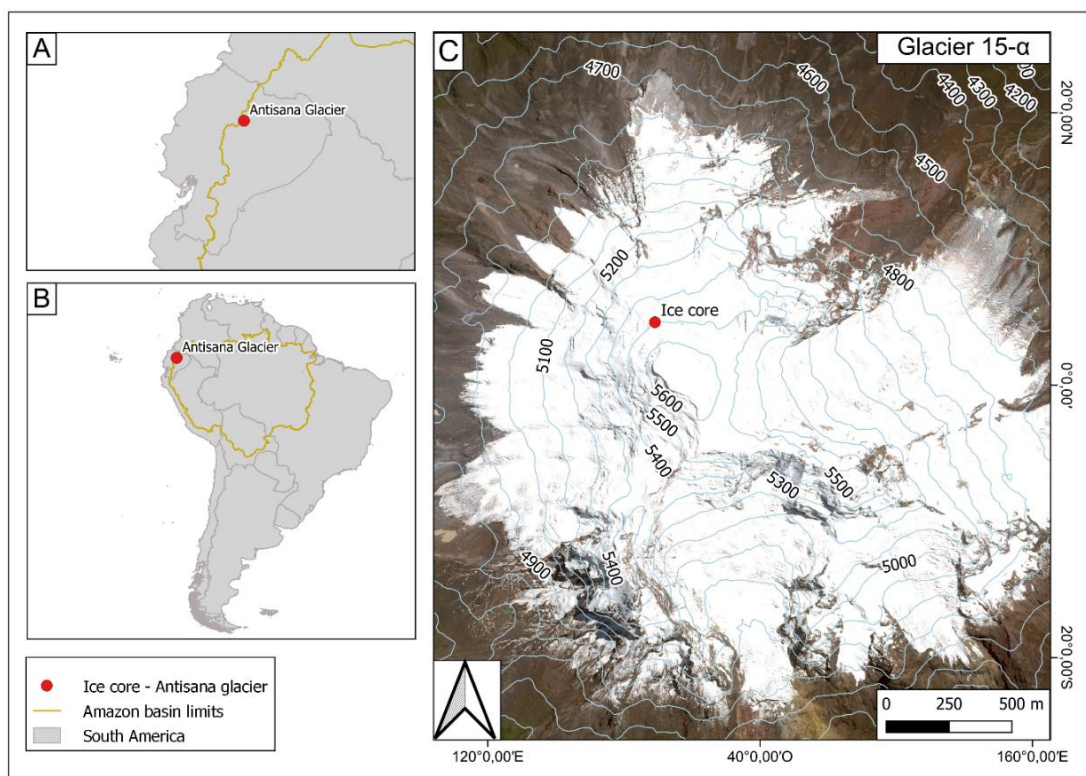


Figure 1 Study area map A) Antisana Volcano is located in Ecuador. B) Runoff from Antisana glacier contributes to the river system of the Amazon River basin. C) Detailed image of glacier 15- α of Antisana Volcano, showing the location where the ice core was extracted at 5520 m.a.s.l.

2.2 Sample collection

In February 2020, an 8-meter-long ice core was extracted from glacier 15- α on Antisana Volcano. This core was recovered at an altitude of 5520 m.a.s.l and 50 samples were taken along the core. The sampling resolution was uneven but covered ranges varying between 8 and 30 cm. The samples were stored in sealed plastic bags. To rule out MPs contamination, the bags were previously rinsed three times with pre-filtered Milli-Q water and air-dried at room temperature to be used as control blanks. The blanks were filled with Milli-Q water, frozen at -18°C , and filtered to quantify and exclude MPs that have been found before from our results. The samples were transported in coolers with dry ice to prevent melting and were stored at -18°C in the refrigerator at the Laboratorio Nacional de Referencia del Agua (LNRA) at the Universidad Regional Amaz3nica Ikiam in Ecuador.

2.3 Polymer characterization

Identification of composition were made by a Fourier transform infrared spectroscopy (FTIR) using the Perkin Elmer Micro-FTIR Spotlight 400 spectrophotometer in reflectance mode and the Spectrum Image software from Perkin Elmer. Of the 50 samples obtained from the ice core, 15 were selected for polymer characterization analysis using FTIR. The criterion for selecting these 15 samples was that they contained the least amount of visible organic matter. The remaining samples were used for the visual quantification of MPs.

FTIR measurements were performed for the composition of the MPs, generating a spectrum for each particle analyzed. The settings selected for both background and infrared images are as follows: Resolution: 32 cm^{-1} , Scans per pixel: 90 (in background) and 8 in samples, Interferometer speed: 2.2 cm s^{-1} , Spectral range: $4000\text{-}650\text{ cm}^{-1}$. A similar number of particles was selected in each filter analyzed, and the spectra obtained were compared with the polymer spectra library and the type of MPs was determined when the match rate was higher than 0.7 (Egea-Corbacho, et al. 2023).

2.4 Isolation and quantification of MPs

To prevent sample contamination, only cotton laboratory coats and garments were used during the MPs isolation in the laboratory. Before each use, all laboratory materials were rinsed three times with pre-filtered Type 1 distilled water. The final rinse water was filtered and used as a blank sample to account for MPs adhered to the materials. To detect airborne MPs contamination during sampling, isolation, and sample quantification, blank filters were placed in open Petri dishes. These filters allowed for the quantification of MPs in the environment and their exclusion from our results. All samples were processed in a fume hood.

For the isolation of MPs, the methodology proposed by Cabrera et al. (2020) and described below was employed. The samples were melted at room temperature, and

250 ml were taken from each melted sample, stored in glass containers, and placed in an oven at 60°C for 2 hours to condense the volume to 50 ml. Subsequently, the samples were mixed with 50 ml of a filtered (0.22 µm) 300 g/L NaCl solution and left to rest for 24 hours, allowing organic particles to separate from the MPs by density.

Once the denser particles had decanted, the samples underwent a vacuum filtration procedure using a borosilicate glass vacuum filtration setup with two different types of membranes: samples prepared for quantifying shapes and sizes were filtered through 0.45 µm cellulose nitrate membranes with a diameter of 47 mm, while samples for quantifying composition were filtered through a 0.45 µm silver membrane (25 mm diameter filter) using the same filtration setup. The filter cup walls were rinsed with pre-filtered Type 1 distilled water to prevent loss of adhered MPs. Finally, the silver filters were placed in Petri dishes and dried in an oven at 40 °C for at least 4 hours.

Organic solvents were not used to remove organic particles, as Cabrera et al. (2021) determined that snow surface samples 120 meters away from where the ice core was extracted contain an insignificant amount of organic matter (TOC of 0.5 mg/L, similar to pure water). The filters were stored in Petri dishes and subsequently covered with 2 ml of a 200 mg/L Rose Bengal solution and analyzed under an optical stereomicroscope with a camera (Motic SMZ-171, 10X/Zoom 0.4). Rose Bengal stains all organic particles pink, while MPs retain their original color (Kosuth et al., 2018; Liebezeit & Liebezeit, 2014; Ribeiro et al., 2024). Finally, the silver filters were placed in Petri dishes and dried in the oven at 40 °C for at least 4 hours.

2.5 Age model

To determine the age of the ice core, the age determination method based on $\delta^{18}\text{O}$ isotopic fluctuations proposed by Calero et al. (2022) was used. The central 3 cm of each of the 50 ice core samples were selected, stored in 20 ml borosilicate glass vials, and kept in a refrigerator at 4°C to prevent evaporation and potential $\delta^{18}\text{O}$ enrichment. The

$\delta^{18}\text{O}$ composition of the samples was measured using a triple water vapor isotope analyzer: laser spectroscopy (Los Gatos Research, LNRA-45-EP).

The constant accumulation of snow gradually compresses the ice layers, leading to the densification of the core (Thompson, 2000). As a result, when sampling at a constant depth in the ice core, the time interval between samples increases with depth. To mitigate the effects of compression in the ice core, a logarithmic transformation (LT) was applied to the depth of each isotopic sample. LT was selected because Calero et al. (2022) demonstrated, through R^2 comparisons of logarithmic depth and isotopic sample density, that this transformation is the most optimal for plotting $\delta^{18}\text{O}$ isotopic data in short cores (<15 meters) from Glacier 15- α .

Then, a probability density function was generated using the depths to identify the most common depth interval among all the samples. This function allowed for the determination of the most frequent distance between samples in the entire dataset, with the highest probability of occurrence (26.9 cm). The selected interval was then used to interpolate the isotope data at constant depth intervals, which is required for running a wavelet analysis. The wavelet analysis was conducted to detect the presence of periodic cycles in the transformed isotope data. All data were analyzed using R version 4.1.1.

2.6 Statistical analysis

The accumulation rate of MPs along the ice core was estimated using the equation of the line from a linear regression. The assumption of normality was evaluated using Shapiro-Wilk tests and a Q-Q plot. No significant differences were considered as the test statistic was $w=0.881$ and the p-value was 0.0013. A Bootstrap analysis was performed with 500 resamplings, where in each iteration, 15 data points were randomly selected from the total of 35 available untransformed samples. For each dataset, a linear regression model was fitted and these were plotted along with the average regression line of the 35 samples (Figure 2) to demonstrate that even when randomly selecting 15

data points, the regression line of these data points approximates the average regression line of all the samples. The equation of the average regression line was obtained, and the rate at which MPs increase with depth was estimated. The statistical analyses were conducted using R software version 4.1.1.

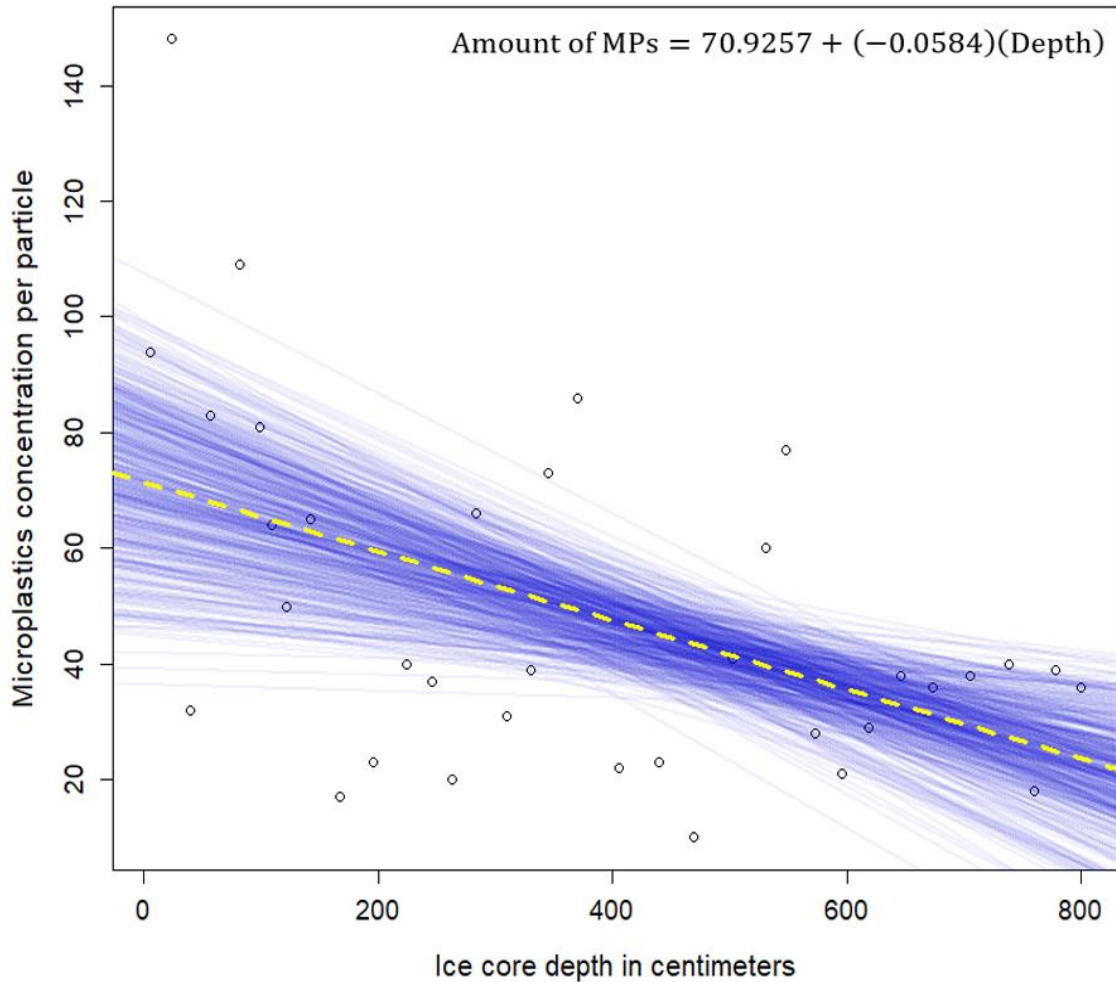


Figure 2. Linear Regression Plot. The blue lines represent the linear regressions resulting from 500 bootstraps and the yellow line represents the average regression between ice depth and MPs concentration. The white points represent the MPs concentrations per particle in the 35 samples.

3. RESULTS.

3.1 Ice core age

Interpolation was performed because wavelet analysis requires data with a constant temporal resolution. To carry out this interpolation, the most common depth interval between consecutive samples, which was 26.9 cm, was chosen to minimize the number of points to be interpolated. It is important to note that interpolation was applied to the log-transformed data. To determine the interpolation resolution (depth), the probability density function graph (Figure 3) was used. On this graph, the highest probability, indicated by the vertical red line at 0.033, was selected as the interpolation resolution for the entire dataset on the x-axis. Thus, the isotope data was interpolated with a depth resolution of 0.033.

A wavelet analysis was performed using the isotopic data with a constant temporal resolution (LT data 0.033), as shown in the heat map of Figure 4. The heat map shows a cone of influence with unusable regions in a white mask and with bright colors the usable areas. Within the cone of influence the colors yellow, green, and blue represent non-significant periodicities, while the red areas surrounded by a thin white line indicate significantly high periodicities. The regions of greatest importance within the significant areas are marked by horizontal black lines, whose periodicity is shown on the y-axis. Note that the non-parallel lines indicate periodicities that increase or decrease in frequency.

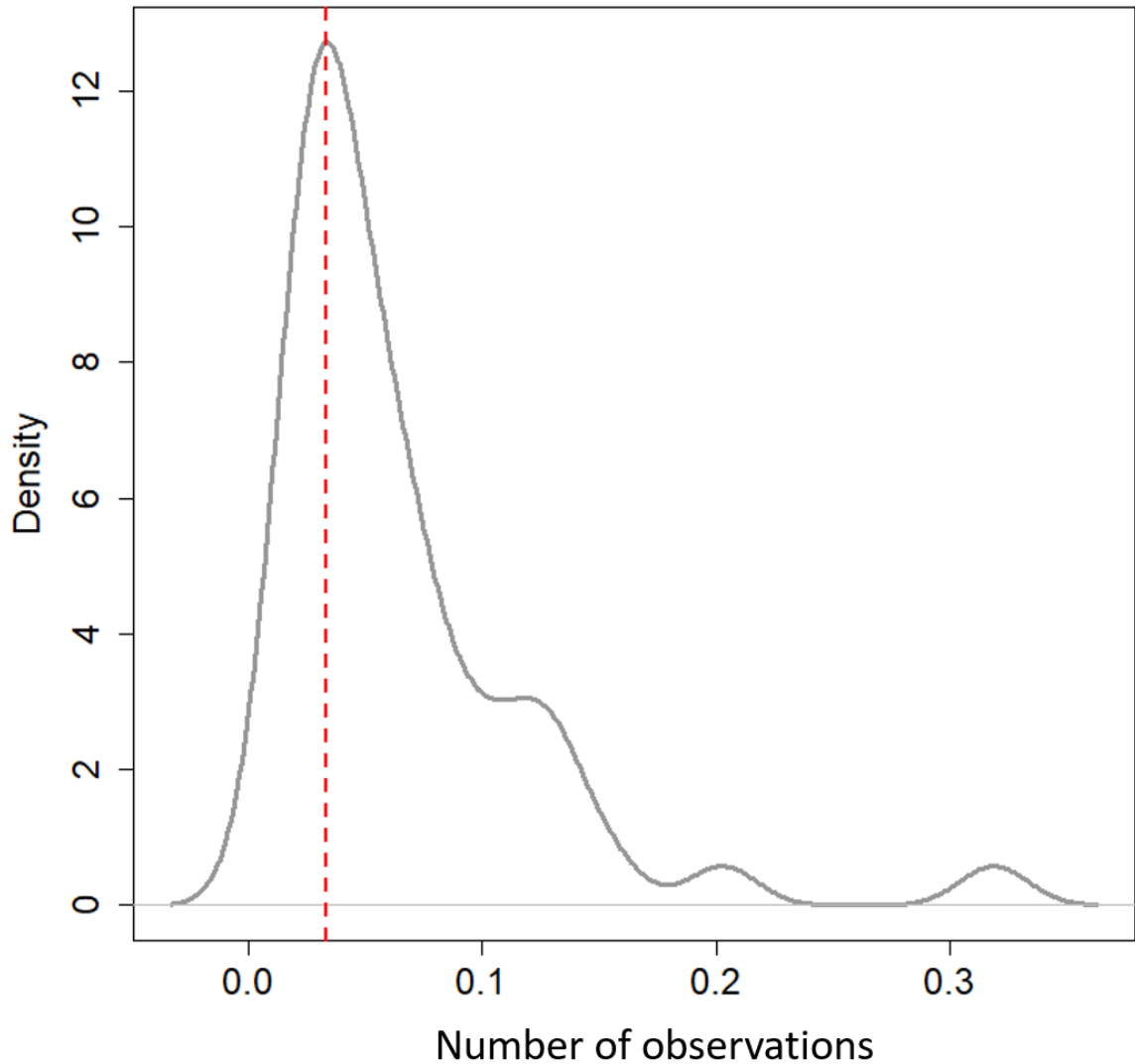


Figure 3. Depth resolution resampling process. The figure depicts a probability density function (y-axis) applied to the LT corrected depths (x-axis). The vertical red line depicts the depth interval (0.033) with the highest probability in the dataset (highest peaks in the figure).

The wavelet analysis identified a significant periodicity with an average wavelet power of 128, represented by a peak in the right panel of Figure 3. This indicates that, on average, a cycle is completed every 128 observations. However, the heat map shows a narrow cone of influence right at 128 step-times, resulting in an unclear isotopic signal. This could be due to the short length of the 8-meter ice core and problems that occurred during sampling. This signal suggests approximately one and a quarter cycles (16 months) of ice accumulation.

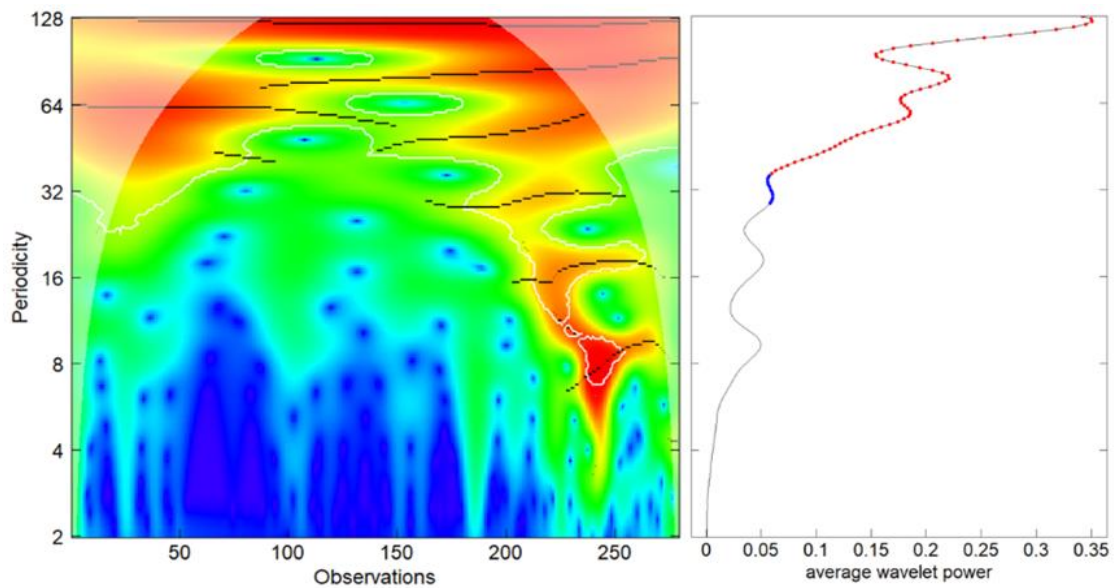


Figure 4. Wavelet Analysis. The heatmap (left image) represents the time-frequency space, with the X-axis for frequency and the Y-axis for periodicity. The black lines in the heatmap indicate confidence contours, marking areas where the detected signals are statistically significant.

To perform a proper wavelet analysis, it is likely that an ice core longer than 8 meters is required, which would allow for the capture of more than one complete cycle for evaluation. However, the extreme conditions at altitudes above 5500 m.a.s.n, where our core was collected, limited the number of samples we could obtain. Despite these limitations, to minimize potential errors in estimating annual cycles, we decided to compare the $\delta^{18}\text{O}$ data obtained from the 8-meter core from the Antisana glacier (this study) with data from a 16.5-meter core extracted from the Chimborazo glacier in 1999 (Ginot et al., 2010).

Ginot et al. (2010) explained that, due to the proximity to the equator, air temperatures remain relatively constant throughout the year. As a result, temperature does not significantly influence the seasonal pattern of stable isotopes. However, the annual peaks of $\delta^{18}\text{O}$ observed in the tropical Andean glaciers are attributed to the annual variation in precipitation which, due to the change of wet and dry seasons, $\delta^{18}\text{O}$ peaks lower than -18‰ are recorded, allowing the identification of a hydrological year in the precipitation.

To visually compare the $\delta^{18}\text{O}$ isotopic peaks, a logarithmic transformation of the depths of the glacial ice cores was performed. Figure 5 reveals that the glacial cores indeed exhibit $\delta^{18}\text{O}$ peaks in the range of -18‰ to -20‰ (represented by the horizontal yellow lines), delineating a hydrological year. For the case of Antisana, these peaks occur in the depth range of 1.85 to 2.95 LT. The reason for choosing to visually compare these glaciers, despite differences in extraction years and core lengths, is the availability of data we have. Furthermore, Calero et al. (2022) has already demonstrated the high correlation between the $\delta^{18}\text{O}$ isotopic data from the Antisana and Chimborazo glaciers.

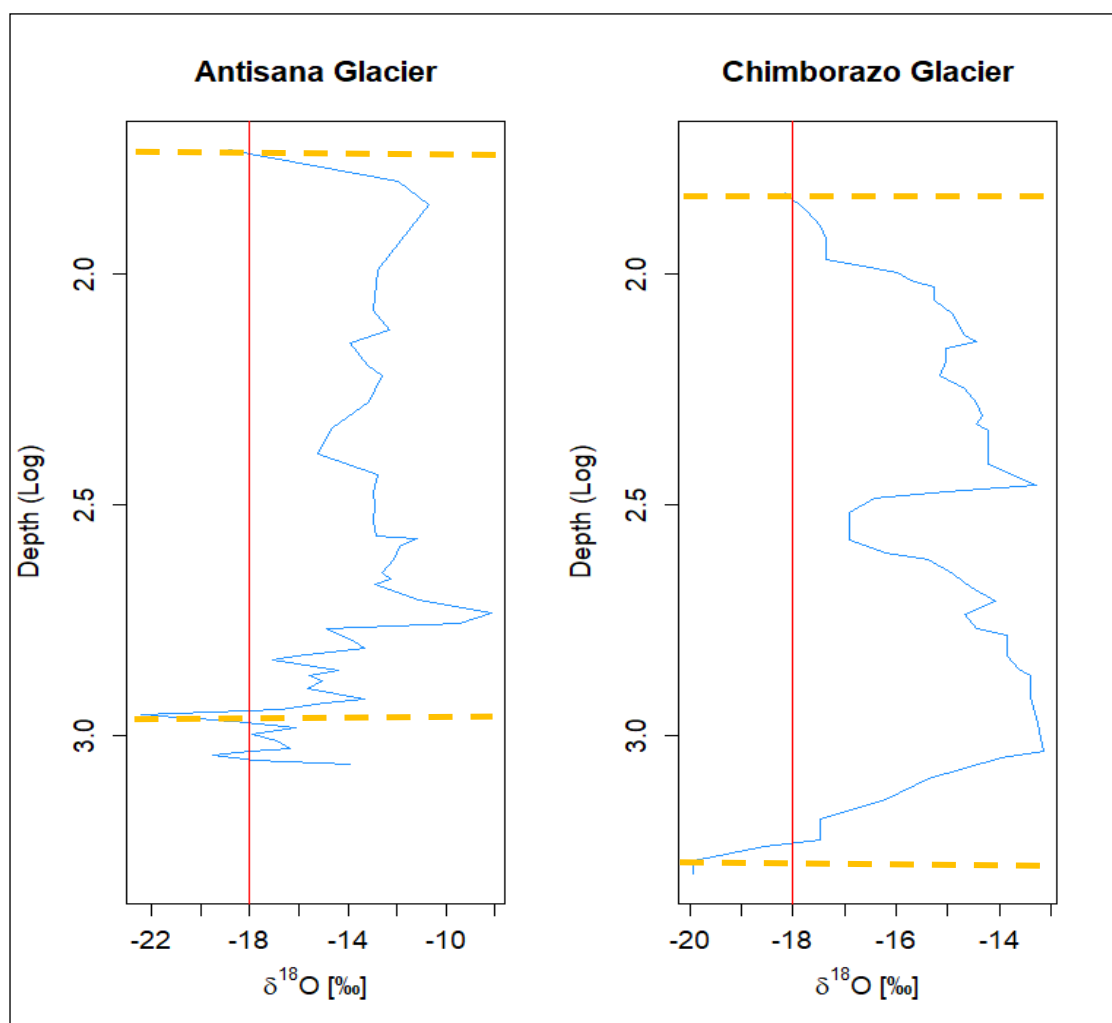


Figure 5. Graph of isotopic fluctuations of $\delta^{18}\text{O}$ plotted against depth in logarithms. The X-axis represents the concentrations of $\delta^{18}\text{O}$ in ‰, while the Y-axis denotes depth in logarithms. Isotopic peaks exist within a range greater than -18‰ that are due to the annual distribution of precipitation, with wet and dry seasons thus delimiting a hydrological year.

3.2 Identification and quantification of MPs

A total of 1762 MPs were visually quantified from the 35 samples throughout the entire ice core. The microplastics were classified according to their shape and polymer type. Based on their shape, the presence of fibers (Figure 6, sections a, b, and c) and fragments (Figure 6, sections d, e, and f) was recorded. The polymers identified in this study included Polyethylene (PE, 28.6%), Propylamine (PMA, 28.6%), Copolymers of 2-(dimethylamino)ethyl methacrylate (PDMAEMA, 14.29%), Polyester (PS, 9.52%), Polyethylenimine (PEI, 4.76%), Polyamide (PA, 4.76%), Polytetrafluoroethylene (PTFE, 4.76%), and Cellulosic Polymers (4.76%) (Figure 7, section a). It was estimated that 67.74% of the 1762 particles quantified along the ice core were fibers, while fragments accounted for 32.26% (Figure 7, section b). Note that the contamination of MPs in the control blanks was less than 10% of the contamination visually detected in the ice core samples. The results showed an increase in the amount of microplastics, both fibers and fragments, as the ice core depth decreased. Fibers increased from 20 to 63 particles (Figure 8, section a) and fragments from 6 to 25 particles (Figure 8, section b), indicating greater accumulation in the more superficial layers.

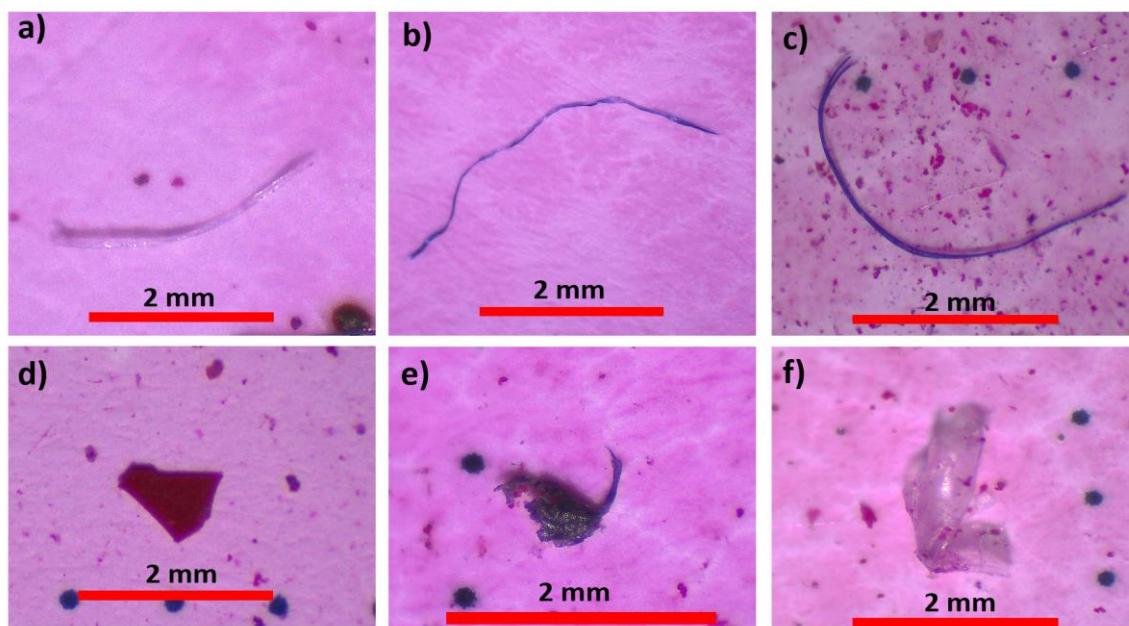


Figure 6. Classification of MPs by shape. a) Transparent fiber, b) blue fiber, c) blue fiber, d) red fragment, e) black fragment, f) transparent fragment.

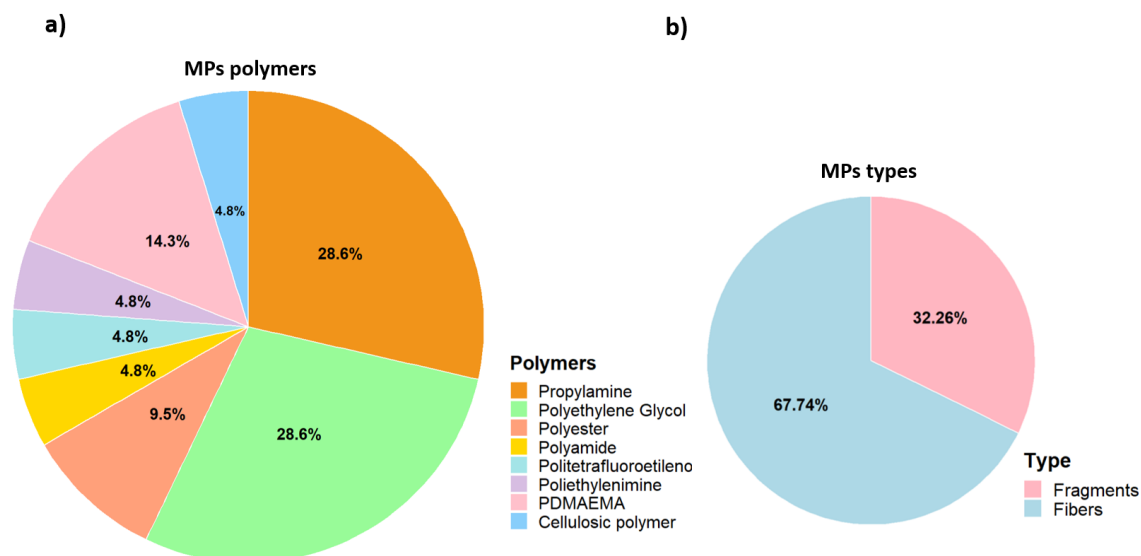


Figure 7. Clasification and proportion of MPs by polymers and shape type. a) Percentage of polymers found along the ice core. b) Percentage of fibers and fragments of MPs recorded in the ice core.

3.3 MPs accumulation rate over time

The trend in the increase of MPs was graphically represented as a function of ice core depth (Figure 2). Isotopic peak analysis (Figure 5) allowed for the identification of samples corresponding to a hydrological year. The results show that, within the logarithmic depth range of 1.85 to 2.95, which covers one hydrological year, the number of MPs increased from 36 particles at the beginning of the year to 83 particles at the end, representing an increase of 47 MPs. The accumulation rate of MPs is represented by the trendline equation for the 35 samples (Figure 2), which is:

$$\text{Amount of MPs} = 70.9257 + (-0.0584)(\text{Depth})$$

In this equation, the coefficient -0.0584 represents the slope, which indicates the change in the amount of MPs in response to changes in depth. Specifically, a slope of -0.0584 means that for each additional unit of depth, the amount of MPs decreases by 0.0584 units. This reflects an inverse relationship between MPs and depth: MPs are increasing at a rate of 5.84% per year of continuous snow accumulation.

4. DISCUSSION

This study estimated the accumulation rate of MPs over a hydrological year using an 8-meter ice core from the 15- α Glacier on the Antisana Volcano in Ecuador. The accumulation rate, represented by the slope of the trendline equation (Figure 2) $\text{Amount of MPs} = 70.9257 + (-0.0584)(\text{Depth})$ indicates that atmospheric MPs accumulate in remote areas like high mountain glaciers at a rate of 5.84% per year. From the 35 samples taken along the ice core, 1762 MPs were visually quantified, showing an increase from 36 to 83 particles over 12 months, indicating that the number of MPs more than doubled within a year. Notably, the controls revealed less than 10% contamination, confirming the reliability of the sample analysis.

Paleoclimatic records obtained from Andean ice cores show that the Atlantic Ocean is their main source of moisture (Ginot et al., 2010; Stansell et al., 2023; Vimeux et al., 2005; Vuille, 2023). The deposition of MPs in tropical Andean glaciers like Antisana implies that MPs are incorporated into the long-distance moisture transport that begins in the Atlantic (Cabrera et al., 2022). Furthermore, as air masses traverse the Amazon rainforest, recurrent precipitation removes certain suspended particles from the atmosphere, including microplastics (Baker and Fritz, 2015; Laraque et al., 2007; Thompson, 2000). This process causes many microplastics to be trapped in the Amazon rainforest, reducing the amount that ultimately reaches the glaciers. However, our results indicate a high annual accumulation rate of microplastics compared to other environments.

Comparing our results with global projections by Lebreton et al. (2019) for MPs accumulation on the ocean surface, we observed significant differences in growth rates. MPs in the atmosphere increased approximately 2.3 times (from 36 to 83 particles) between 2021 and 2022, while oceanic MPs grew by only 1.05 times (from 594,000 to 629,300 tons) in the same period (Figure 8). Atmospheric transfer of MPs is notably faster than aquatic transfer, enabling long-distance transport to remote areas without

nearby sources of pollution. This could be due to smaller, less dense MPs being more easily carried by wind, while larger MPs remain longer in coastal areas and thus undergo fragmentation until they have the characteristics to be transported by air or water current (Hinata et al., 2023).

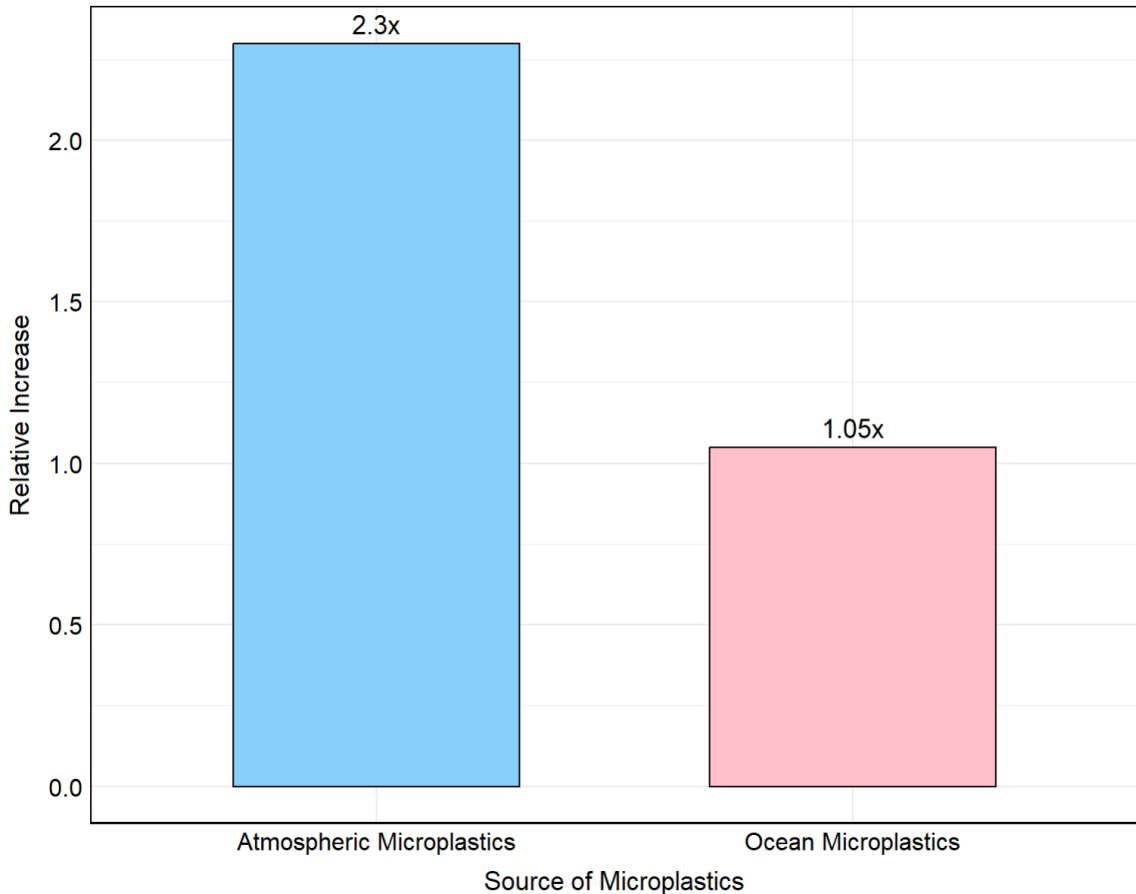


Figure 8. Differences between the growth rates of atmospheric MPs quantified in this research and the Lebreton model data on the increase of MPs in the ocean. The amount of MPs in the atmosphere multiplied approximately by 2.3 from its initial value, while the amount of MPs in the ocean multiplied by 1.05 from its initial value.

It was determined that the most common form of MPs were fibers (67.74%), followed by fragments (32.26%) of the total 1762 visually quantified particles. This proportion may be due to fibers having a higher surface area relative to their volume and being less dense than other forms of MPs, allowing them to be transported over greater distances (Zuo et al., 2024). Density plays a significant role in the long-distance transport of particles like microfibers (Cai et al., 2015). Fibers have also been characterized as the

most common form of MPs in mountain ranges such as the Alps and Andes (Cabrera et al., 2020, Napper et al., 2020; Parolini et al., 2021). This recurrence may be due to fibers being the most common type of MPs used in the textile industry, constituting a large part of primary MPs. The increase in fiber production over time is linked to the growth of synthetic textile manufacturing, which is estimated to have a growth rate of 6.6% between 2021 and 2028 due to the growing demand for polyester (Gao et al., 2024).

Fragments were found to be the second most common type of MPs among the 1762 particles counted. Fragments originate from the breakdown of larger plastic items (Pinlova & Nowack, 2024) and can be transported to remote areas. Unlike fibers, which easily travel through the air due to their low density, fragments undergo a more extensive segmentation process before becoming small enough to be transported via water and air. Irregularly shaped MP fragments can get trapped in porous materials due to their uneven surface (Dong et al., 2021, 2022), which could contribute to the higher presence of microfibers in the atmosphere.

The polymers identified in the 15 samples analyzed with FTIR included Polyethylene (PE, 28.6%), Propylamine (PMA, 28.6%), 2-(dimethylamino)ethyl methacrylate copolymers (PDMAEMA, 14.29%), Polyester (PS, 9.52%), Polyethylenimine (PEI, 4.76%), Polyamide (PA, 4.76%), Polytetrafluoroethylene (PTFE, 4.76%), and Cellulosic polymers (4.76%). The results of the polymer type analysis using FTIR determined that there was a higher concentration of polymers like propylamine (PMA) and polyethylene glycol (PE), which may be related to the rapid expansion of the packaging and textile industries. PE is the predominant material in food packaging (Cheshmazar et al., 2021; Isci & Dagdemir, 2024). However, PE includes substances such as antimony, lead, and phthalate esters, which cause issues in human reproduction, allergies/asthma, and carcinogenicity (Ulanova et al., 2019, Vernet et al., 2017, Jeddi et al., 2016).

Finally, the annual accumulation rate of MPs on the Antisana glacier is increasing at a rate of 5.84%. This rise reflects the growing presence of MPs in the atmosphere and in the air we breathe, although in different proportions compared to the ice core. It is

important to note that the MPs we are currently recording originate from plastics released into the environment before the 1970s (Lebrenton et al., 2019), and therefore, the amount of MPs will increase exponentially in the coming years. The deposition of MPs on tropical glaciers contributes to the contamination of rivers such as the Amazon and may reduce the snow albedo, accelerating glacier melt (Kang et al., 2019). This melting will increase MP contamination in meltwater, affecting water quality in areas like Quito. A more detailed assessment of the transport and accumulation of MPs in other aquatic environments is required to improve estimates of when MPs will become harmful to human health.

5. CONCLUSION

This study confirms that the amount of MPs in the Antisana Glacier is inversely proportional to the depth of the ice core. That is, MP accumulation indeed increases as the ice is deposited, as evidenced by an annual accumulation rate of 5.84%. This finding indicates that MPs in the atmosphere accumulate in remote areas such as high mountain glaciers and increase in the air we breathe. Over the studied year, the amount of MPs in the ice core more than doubled, rising from 36 to 83 particles.

Comparisons with global projections reveal that atmospheric transport of MPs occurs at a much faster rate than oceanic transport, suggesting considerable long-distance transport capability. Moreover, the predominant MPs are fibers, linked to the textile industry, and fragments resulting from the breakdown of larger plastics. The deposition of MPs in tropical glaciers contributes to the contamination of rivers like the Amazon and can reduce snow albedo, accelerating glacier melt. This increase in melting may intensify MPs contamination in meltwater, affecting water quality in areas such as Quito. It is important to note that the MPs currently recorded originate from plastics released before the 1970s, and accumulation rates are expected to continue rising. While the consequences are not yet fully understood, further studies on the transport and accumulation of MPs in different environments are crucial to better assess their potential impacts on human health and the environment.

6. REFERENCES

- Allen, S., Allen, D., Baladima, F., Phoenix, V. R., Thomas, J. L., Le Roux, G., & Sonke, J. E. (2021). Evidence of free tropospheric and long-range transport of microplastic at Pic du Midi Observatory. *Nature Communications*, *12*(1). <https://doi.org/10.1038/s41467-021-27454-7>
- Allen, S., Allen, D., Phoenix, V. R., Le Roux, G., Durántez Jiménez, P., Simonneau, A., Binet, S., & Galop, D. (2019). Atmospheric transport and deposition of microplastics in a remote mountain catchment. *Nature Geoscience*, *12*(5), 339–344. <https://doi.org/10.1038/s41561-019-0335-5>
- Ambrosini, R., Azzoni, R. S., Pittino, F., Diolaiuti, G., Franzetti, A., & Parolini, M. (2019). First evidence of microplastic contamination in the supraglacial debris of an alpine glacier. *Environmental Pollution*, *253*, 297–301. <https://doi.org/10.1016/j.envpol.2019.07.005>
- Andrady, A. L. (2011). Microplastics in the marine environment. In *Marine Pollution Bulletin* (Vol. 62, Issue 8, pp. 1596–1605). <https://doi.org/10.1016/j.marpolbul.2011.05.030>
- Baker, P. A., & Fritz, S. C. (2015). Nature and causes of Quaternary climate variation of tropical South America. In *Quaternary Science Reviews* (Vol. 124, pp. 31–47). Elsevier Ltd. <https://doi.org/10.1016/j.quascirev.2015.06.011>
- Bank, M. S., & Hansson, S. V. (2019). The Plastic Cycle: A Novel and Holistic Paradigm for the Anthropocene. In *Environmental Science and Technology* (Vol. 53, Issue 13, pp. 7177–7179). American Chemical Society. <https://doi.org/10.1021/acs.est.9b02942>
- Barceló, D., Picó, Y., & Alfarhan, A. H. (2023). Microplastics: Detection in human samples, cell line studies, and health impacts. *Environmental Toxicology and Pharmacology*, *101*. <https://doi.org/10.1016/j.etap.2023.104204>
- Barnes, D. K. A., Galgani, F., Thompson, R. C., & Barlaz, M. (2009). Accumulation and fragmentation of plastic debris in global environments. *Philosophical Transactions of the Royal Society B: Biological Sciences*, *364*(1526), 1985–1998. <https://doi.org/10.1098/rstb.2008.0205>
- Basantes-Serrano, R., Rabatel, A., Francou, B., Vincent, C., Maisincho, L., Cáceres, B., Galarraga, R., & Alvarez, D. (2016). Slight mass loss revealed by reanalyzing glacier mass-balance observations on Glaciar Antisana 15 α (inner tropics) during the 1995-2012 period. *Journal of Glaciology*, *62*(231), 124–136. <https://doi.org/10.1017/jog.2016.17>

- Bergmann, M., Mützel, S., Primpke, S., Tekman, M. B., Trachsel, J., & Gerdt, G. (2019). White and wonderful? Microplastics prevail in snow from the Alps to the Arctic. *Science Advances*, 5(8). <https://doi.org/10.1126/sciadv.aax1157>
- Brahney, J., Hallerud, M., Heim, E., Hahnenberger, M., & Sukumaran, S. (n.d.). *Plastic rain in protected areas of the United States*. <http://science.sciencemag.org/>
- Brahney, J., Mahowald, N., Prank, M., Cornwell, G., Klimont, Z., Matsui, H., & Prather, K. A. (n.d.). *Constraining the atmospheric limb of the plastic cycle*. <https://doi.org/10.1073/pnas.2020719118/-/DCSupplemental>
- Cabrera, M., Moulatlet, G. M., Valencia, B. G., Maisincho, L., Rodríguez-Barroso, R., Albendín, G., Sakali, A., Lucas-Solis, O., Conicelli, B., & Capparelli, M. V. (2022). Microplastics in a tropical Andean Glacier: A transportation process across the Amazon basin? *Science of the Total Environment*, 805. <https://doi.org/10.1016/j.scitotenv.2021.150334>
- Cabrera, M., Valencia, B. G., Lucas-Solis, O., Calero, J. L., Maisincho, L., Conicelli, B., Massaine Moulatlet, G., & Capparelli, M. V. (2020). A new method for microplastic sampling and isolation in mountain glaciers: A case study of one antisana glacier, Ecuadorian Andes. *Case Studies in Chemical and Environmental Engineering*, 2. <https://doi.org/10.1016/j.cscee.2020.100051>
- Cauvy-Fraunié, S., Condom, T., Rabatel, A., Villacis, M., Jacobsen, D., & Dangles, O. (2013). Technical Note: Glacial influence in tropical mountain hydrosystems evidenced by the diurnal cycle in water levels. *Hydrology and Earth System Sciences*, 17(12), 4803–4816. <https://doi.org/10.5194/hess-17-4803-2013>
- Chandra, S., & Walsh, K. B. (2024). Microplastics in water: Occurrence, fate and removal. In *Journal of Contaminant Hydrology* (Vol. 264). Elsevier B.V. <https://doi.org/10.1016/j.jconhyd.2024.104360>
- Chandranathan, K., Fraser, M. P., & Herckes, P. (2024). Microplastics are ubiquitous and increasing in soil of a sprawling urban area, Phoenix (Arizona). *Science of the Total Environment*, 906. <https://doi.org/10.1016/j.scitotenv.2023.167617>
- Cheshmazar, E., Arfaeina, L., Vasseghian, Y., Ramavandi, B., Moradi, M., Hashemi, S. E., Asgari, E., Arfaeina, H., Dragoi, E. N., & Mousavi Khaneghah, A. (2021). Phthalate acid esters in pickled vegetables packaged in polyethylene terephthalate container: Occurrence, migration, and estrogenic activity-associated risk assessment. *Journal of Food Composition and Analysis*, 99. <https://doi.org/10.1016/j.jfca.2021.103880>
- Cole, M., Lindeque, P. K., Fileman, E., Clark, J., Lewis, C., Halsband, C., & Galloway, T. S. (2016). Microplastics Alter the Properties and Sinking Rates of Zooplankton Faecal Pellets.

- Environmental Science and Technology*, 50(6), 3239–3246.
<https://doi.org/10.1021/acs.est.5b05905>
- Dhivert, E., Pruvost, J., Winiarski, T., Gasperi, J., Delor-Jestin, F., Tassin, B., & Mourier, B. (2024). Time-varying microplastic contributions of a large urban and industrial area to river sediments. *Environmental Pollution*, 347. <https://doi.org/10.1016/j.envpol.2024.123702>
- Ding, J., Sun, C., He, C., Zheng, L., Dai, D., & Li, F. (2022). Atmospheric microplastics in the Northwestern Pacific Ocean: Distribution, source, and deposition. *Science of the Total Environment*, 829. <https://doi.org/10.1016/j.scitotenv.2022.154337>
- Dissanayake, P. D., Kim, S., Sarkar, B., Oleszczuk, P., Sang, M. K., Haque, M. N., Ahn, J. H., Bank, M. S., & Ok, Y. S. (2022). Effects of microplastics on the terrestrial environment: A critical review. *Environmental Research*, 209. <https://doi.org/10.1016/j.envres.2022.112734>
- Dong, S., Xia, J., Sheng, L., Wang, W., Liu, H., & Gao, B. (2021). Transport characteristics of fragmental polyethylene glycol terephthalate (PET) microplastics in porous media under various chemical conditions. *Chemosphere*, 276. <https://doi.org/10.1016/j.chemosphere.2021.130214>
- Dong, S., Zhou, M., Su, X., Xia, J., Wang, L., Wu, H., Suakollie, E. B., & Wang, D. (2022). Transport and retention patterns of fragmental microplastics in saturated and unsaturated porous media: A real-time pore-scale visualization. *Water Research*, 214. <https://doi.org/10.1016/j.watres.2022.118195>
- Evangelidou, N., Grythe, H., Klimont, Z., Heyes, C., Eckhardt, S., Lopez-Aparicio, S., & Stohl, A. (2020). Atmospheric transport is a major pathway of microplastics to remote regions. *Nature Communications*, 11(1). <https://doi.org/10.1038/s41467-020-17201-9>
- Fox, S., Stefánsson, H., Peternell, M., Zlotkiy, E., Ásbjörnsson, E. J., Sturkell, E., Wanner, P., & Konrad-Schmolke, M. (2024). Physical characteristics of microplastic particles and potential for global atmospheric transport: A meta-analysis. In *Environmental Pollution* (Vol. 342). Elsevier Ltd. <https://doi.org/10.1016/j.envpol.2023.122938>
- Gao, M., Yang, T., Som, C., & Nowack, B. (2024). Differences in the release of microplastic fibers and fibrils from virgin and recycled polyester textiles. *Resources, Conservation and Recycling*, 207. <https://doi.org/10.1016/j.resconrec.2024.107659>
- George, M., Nallet, F., & Fabre, P. (2024). A threshold model of plastic waste fragmentation: New insights into the distribution of microplastics in the ocean and its evolution over time. *Marine Pollution Bulletin*, 199. <https://doi.org/10.1016/j.marpolbul.2023.116012>
- Geyer, R., Jambeck, J. R., & Law, K. L. (2017). *Production, use, and fate of all plastics ever made*. <http://advances.sciencemag.org/>

- Ginot, P., Schotterer, U., Stichler, W., Godoi, M. A., Francou, B., & Schwikowski, M. (2010). Influence of the Tungurahua eruption on the ice core records of Chimborazo, Ecuador. *Cryosphere*, 4(4), 561–568. <https://doi.org/10.5194/tc-4-561-2010>
- Gonzalez-Pleiter, M., Lacerot, G., Edo, C., Pablo Lozoya, J., Legane´s, F., Fernández-Pinãs, F., Rosal, R., & Teixeira-De-Mello, F. (2021). A pilot study about microplastics and mesoplastics in an Antarctic glacier. *Cryosphere*, 15(6), 2531–2539. <https://doi.org/10.5194/tc-15-2531-2021>
- Habibi, N., Uddin, S., Behbehani, M., & Lee, J. Y. (2024). Is atmospheric pathway a significant contributor to microplastics in the marine environment? *Emerging Contaminants*, 10(2). <https://doi.org/10.1016/j.emcon.2023.100297>
- Habibi, N., Uddin, S., Fowler, S. W., & Behbehani, M. (2022). Microplastics in the atmosphere: a review. In *Journal of Environmental Exposure Assessment* (Vol. 1, Issue 1). OAE Publishing Inc. <https://doi.org/10.20517/jeea.2021.07>
- Hall, M. L., Mothes, P. A., Samaniego, P., Militzer, A., Beate, B., Ramón, P., & Robin, C. (2017). Antisana volcano: A representative andesitic volcano of the eastern cordillera of Ecuador: Petrography, chemistry, tephra and glacial stratigraphy. *Journal of South American Earth Sciences*, 73, 50–64. <https://doi.org/10.1016/j.jsames.2016.11.005>
- Hinata, H., Kuwae, M., Tsugeki, N., Masumoto, I., Tani, Y., Hatada, Y., Kawamata, H., Mase, A., Kasamo, K., Sukenaga, K., & Suzuki, Y. (2023). A 75-year history of microplastic fragment accumulation rates in a semi-enclosed hypoxic basin. *Science of the Total Environment*, 854. <https://doi.org/10.1016/j.scitotenv.2022.158751>
- Hurley, R., Woodward, J., & Rothwell, J. J. (2018). Microplastic contamination of river beds significantly reduced by catchment-wide flooding. *Nature Geoscience*, 11(4), 251–257. <https://doi.org/10.1038/s41561-018-0080-1>
- Isci, G., & Dagdemir, E. (2024). Human health risk assessment of phthalate esters and antimony levels in beverages packaged in polyethylene terephthalate under different storage conditions. *Journal of Food Composition and Analysis*, 126. <https://doi.org/10.1016/j.jfca.2023.105922>
- Janakiram, R., Keerthivasan, R., Janani, R., Ramasundaram, S., Martin, M. V., Venkatesan, R., Ramana Murthy, M. V., & Sudhakar, T. (2023). Seasonal distribution of microplastics in surface waters of the Northern Indian Ocean. *Marine Pollution Bulletin*, 190. <https://doi.org/10.1016/j.marpolbul.2023.114838>
- Kang, S., Zhang, Q., Qian, Y., Ji, Z., Li, C., Cong, Z., Zhang, Y., Guo, J., Du, W., Huang, J., You, Q., Panday, A.K., Rupakheti, M., Chen, D., Gustafsson, Ö., Thiemens, M.H., Qin, D., 2019. Linking atmospheric pollution to cryospheric change in the third pole region: current

- progress and future prospects. *Natl. Sci. Rev.* 6 (4), 796–809. <https://doi.org/10.1093/nsr/nwz031>
- Khoshmanesh, M., Sanati, A. M., & Ramavandi, B. (2023). Co-occurrence of microplastics and organic/inorganic contaminants in organisms living in aquatic ecosystems: A review. In *Marine Pollution Bulletin* (Vol. 187). Elsevier Ltd. <https://doi.org/10.1016/j.marpolbul.2022.114563>
- Kosuth, M., Mason, S. A., & Wattenberg, E. V. (2018). Anthropogenic contamination of tap water, beer, and sea salt. *PLoS ONE*, 13(4). <https://doi.org/10.1371/journal.pone.0194970>
- Koutnik, V. S., Leonard, J., Alkidim, S., DePrima, F. J., Ravi, S., Hoek, E. M. V., & Mohanty, S. K. (2021). Distribution of microplastics in soil and freshwater environments: Global analysis and framework for transport modeling. In *Environmental Pollution* (Vol. 274). Elsevier Ltd. <https://doi.org/10.1016/j.envpol.2021.116552>
- Kwon, G., Cho, D. W., Park, J., Bhatnagar, A., & Song, H. (2023). A review of plastic pollution and their treatment technology: A circular economy platform by thermochemical pathway. In *Chemical Engineering Journal* (Vol. 464). Elsevier B.V. <https://doi.org/10.1016/j.cej.2023.142771>
- Laraque, A., Ronchail, J., Cochonneau, G., Pombosa, R., & Guyot, J. L. (2007). Heterogeneous distribution of rainfall and discharge regimes in the Ecuadorian Amazon basin. *Journal of Hydrometeorology*, 8(6), 1364–1381. <https://doi.org/10.1175/2007JHM784.1>
- Liebezeit, G., & Liebezeit, E. (2014). Synthetic particles as contaminants in German beers. *Food Additives and Contaminants - Part A*, 31(9), 1574–1578. <https://doi.org/10.1080/19440049.2014.945099>
- Liu, K., Wang, X., Song, Z., Wei, N., & Li, D. (2020). Terrestrial plants as a potential temporary sink of atmospheric microplastics during transport. *Science of the Total Environment*, 742. <https://doi.org/10.1016/j.scitotenv.2020.140523>
- Liu, K., Wu, T., Wang, X., Song, Z., Zong, C., Wei, N., & Li, D. (2019). Consistent Transport of Terrestrial Microplastics to the Ocean through Atmosphere. *Environmental Science and Technology*, 53(18), 10612–10619. <https://doi.org/10.1021/acs.est.9b03427>
- Liu, Z., Liang, T., & Liu, X. (2024). Characteristics, distribution patterns and sources of atmospheric microplastics in the Bohai and Yellow Seas, China. *Science of the Total Environment*, 926. <https://doi.org/10.1016/j.scitotenv.2024.171906>
- Martina, M., & Trini Castelli, S. (2023). Modelling the Potential Long-Range Dispersion of Atmospheric Microplastics Reaching a Remote Site. *Atmospheric Environment*, 312. <https://doi.org/10.1016/j.atmosenv.2023.120044>

- Materić, D., Kasper-Giebl, A., Kau, D., Anten, M., Greilinger, M., Ludewig, E., Van Sebille, E., Röckmann, T., & Holzinger, R. (2020). Micro-and Nanoplastics in Alpine Snow: A New Method for Chemical Identification and (Semi)Quantification in the Nanogram Range. *Environmental Science and Technology*, 54(4), 2353–2359. <https://doi.org/10.1021/acs.est.9b07540>
- Mierzejewski, K., Kurzyńska, A., Golubska, M., Całka, J., Gałęcka, I., Szabelski, M., Pauksto, L., Andronowska, A., & Bogacka, I. (2023). New insights into the potential effects of PET microplastics on organisms via extracellular vesicle-mediated communication. *Science of the Total Environment*, 904. <https://doi.org/10.1016/j.scitotenv.2023.166967>
- Napper, I. E., Davies, B. F. R., Clifford, H., Elvin, S., Koldewey, H. J., Mayewski, P. A., Miner, K. R., Potocki, M., Elmore, A. C., Gajurel, A. P., & Thompson, R. C. (2020). Reaching New Heights in Plastic Pollution—Preliminary Findings of Microplastics on Mount Everest. *One Earth*, 3(5), 621–630. <https://doi.org/10.1016/j.oneear.2020.10.020>
- Niu, X., Wang, X., Dong, H., Ciren, N., Zhang, H., Chen, X., Zhuoga, S., Jia, X., Xu, L., & Zhou, Y. (2024). Microplastics in remote region of the world: Insights from the glacier of Geladandong, China. *Applied Geochemistry*, 168. <https://doi.org/10.1016/j.apgeochem.2024.106026>
- Otegui, M. B. P., Schuab, J. M., França, M. A., Caniçali, F. B., Yapuchura, E. R., Zamprogno, G. C., & da Costa, M. B. (2024). Microplastic contamination in different shell length in *Tivela mactroides* (Born, 1778). *Science of the Total Environment*, 922. <https://doi.org/10.1016/j.scitotenv.2024.171283>
- Parolini, M., De Felice, B., Lamonica, C., Cioccarelli, S., Crosta, A., Diolaiuti, G., Ortenzi, M. A., & Ambrosini, R. (2021). Macroplastics contamination on glaciers from Italian Central-Western Alps. *Environmental Advances*, 5. <https://doi.org/10.1016/j.envadv.2021.100084>
- Pinlova, B., & Nowack, B. (2024). From cracks to secondary microplastics - surface characterization of polyethylene terephthalate (PET) during weathering. *Chemosphere*, 352. <https://doi.org/10.1016/j.chemosphere.2024.141305>
- Plasticsthefastfacts2023-1*. (n.d.).
- Polidoro, B., Lewis, T., & Clement, C. (2022). A screening-level human health risk assessment for microplastics and organic contaminants in near-shore marine environments in American Samoa. *Heliyon*, 8(3). <https://doi.org/10.1016/j.heliyon.2022.e09101>
- Priya, K. L., Renjith, K. R., Joseph, C. J., Indu, M. S., Srinivas, R., & Haddout, S. (2022). Fate, transport and degradation pathway of microplastics in aquatic environment — A critical review. In *Regional Studies in Marine Science* (Vol. 56). Elsevier B.V. <https://doi.org/10.1016/j.rsma.2022.102647>

- Rafa, N., Ahmed, B., Zohora, F., Bakya, J., Ahmed, S., Ahmed, S. F., Mofijur, M., Chowdhury, A. A., & Almomani, F. (2024). Microplastics as carriers of toxic pollutants: Source, transport, and toxicological effects. In *Environmental Pollution* (Vol. 343). Elsevier Ltd. <https://doi.org/10.1016/j.envpol.2023.123190>
- Ribeiro, F., Duarte, A. C., & da Costa, J. P. (2024). Staining methodologies for microplastics screening. In *TrAC - Trends in Analytical Chemistry* (Vol. 172). Elsevier B.V. <https://doi.org/10.1016/j.trac.2024.117555>
- Rosso, B., Scoto, F., Hallanger, I. G., Larose, C., Gallet, J. C., Spolaor, A., Bravo, B., Barbante, C., Gambaro, A., & Corami, F. (2024). Characteristics and quantification of small microplastics (<100 μm) in seasonal svalbard snow on glaciers and lands. *Journal of Hazardous Materials*, 467. <https://doi.org/10.1016/j.jhazmat.2024.133723>
- Salomone, V. N., Passucci, V., & Areco, M. M. (2023). Microplastic pollution in marine environments: Exploring sources, sinks, and consequences with a focus on algal interactions. In *Regional Studies in Marine Science* (Vol. 68). Elsevier B.V. <https://doi.org/10.1016/j.rsma.2023.103270>
- Scheurer, M., & Bigalke, M. (2018). Microplastics in Swiss Floodplain Soils. *Environmental Science and Technology*, 52(6), 3591–3598. <https://doi.org/10.1021/acs.est.7b06003>
- Song, X., Zhuang, W., Cui, H., Liu, M., Gao, T., Li, A., & Gao, Z. (2022). Interactions of microplastics with organic, inorganic and bio-pollutants and the ecotoxicological effects on terrestrial and aquatic organisms. In *Science of the Total Environment* (Vol. 838). Elsevier B.V. <https://doi.org/10.1016/j.scitotenv.2022.156068>
- Sridharan, S., Kumar, M., Singh, L., Bolan, N. S., & Saha, M. (2021). Microplastics as an emerging source of particulate air pollution: A critical review. In *Journal of Hazardous Materials* (Vol. 418). Elsevier B.V. <https://doi.org/10.1016/j.jhazmat.2021.126245>
- Stansell, N. D., Abbott, M. B., Diaz, M. B., Licciardi, J. M., Mark, B. G., Polissar, P. J., Rodbell, D. T., & Shutkin, T. Y. (2023). Pre-industrial Holocene glacier variability in the tropical Andes as context for anthropogenically driven ice retreat. *Global and Planetary Change*, 229. <https://doi.org/10.1016/j.gloplacha.2023.104242>
- Stegmann, P., Daioglou, V., Londo, M., van Vuuren, D. P., & Junginger, M. (2022). Plastic futures and their CO₂ emissions. *Nature*, 612(7939), 272–276. <https://doi.org/10.1038/s41586-022-05422-5>
- Surendran, U., Jayakumar, M., Raja, P., Gopinath, G., & Chellam, P. V. (2023). Microplastics in terrestrial ecosystem: Sources and migration in soil environment. *Chemosphere*, 318. <https://doi.org/10.1016/j.chemosphere.2023.137946>

- Thompson, L. G. (2000). Ice core evidence for climate change in the Tropics: implications for our future. In *Quaternary Science Reviews* (Vol. 19).
- Vimeux, F., Gallaire, R., Bony, S., Hoffmann, G., & Chiang, J. C. H. (2005). What are the climate controls on δD in precipitation in the Zongo Valley (Bolivia)? Implications for the Illimani ice core interpretation. *Earth and Planetary Science Letters*, 240(2), 205–220. <https://doi.org/10.1016/j.epsl.2005.09.031>
- Vuille, M. (2023). Ice core records from South America. In *Reference Module in Earth Systems and Environmental Sciences*. Elsevier. <https://doi.org/10.1016/b978-0-323-99931-1.00147-1>
- Walker, T. R., & Fequet, L. (2023). Current trends of unsustainable plastic production and micro(nano)plastic pollution. In *TrAC - Trends in Analytical Chemistry* (Vol. 160). Elsevier B.V. <https://doi.org/10.1016/j.trac.2023.116984>
- Wang, X., Li, C., Liu, K., Zhu, L., Song, Z., & Li, D. (2020). Atmospheric microplastic over the South China Sea and East Indian Ocean: abundance, distribution and source. *Journal of Hazardous Materials*, 389. <https://doi.org/10.1016/j.jhazmat.2019.121846>
- Wang, Y., & Chen, X. (2023). Aggregation behavior of polyethylene microplastics in the nearshore environment: The role of particle size, environmental condition and turbulent flow. *Science of the Total Environment*, 901. <https://doi.org/10.1016/j.scitotenv.2023.165941>
- Ward, E., Gordon, M., Hanson, R., & Jantunen, L. M. (2024). Modelling the effect of shape on atmospheric microplastic transport. *Atmospheric Environment*, 326. <https://doi.org/10.1016/j.atmosenv.2024.120458>
- Wright, S. L., Thompson, R. C., & Galloway, T. S. (2013). The physical impacts of microplastics on marine organisms: a review. In *Environmental pollution (Barking, Essex : 1987)* (Vol. 178, pp. 483–492). <https://doi.org/10.1016/j.envpol.2013.02.031>
- Wright, S. L., Ulke, J., Font, A., Chan, K. L. A., & Kelly, F. J. (2020). Atmospheric microplastic deposition in an urban environment and an evaluation of transport. *Environment International*, 136. <https://doi.org/10.1016/j.envint.2019.105411>
- Zhang, Y., Kang, S., Allen, S., Allen, D., Gao, T., & Sillanpää, M. (2020). Atmospheric microplastics: A review on current status and perspectives. In *Earth-Science Reviews* (Vol. 203). Elsevier B.V. <https://doi.org/10.1016/j.earscirev.2020.103118>
- Zuo, C., Li, Y., Chen, Y., Jiang, J., Qiu, W., & Chen, Q. (2024). Leaching of heavy metals from polyester microplastic fibers and the potential risks in simulated real-world scenarios. *Journal of Hazardous Materials*, 461. <https://doi.org/10.1016/j.jhazmat.2023.132639>